SLOW EARTHQUAKES

Newsletter05

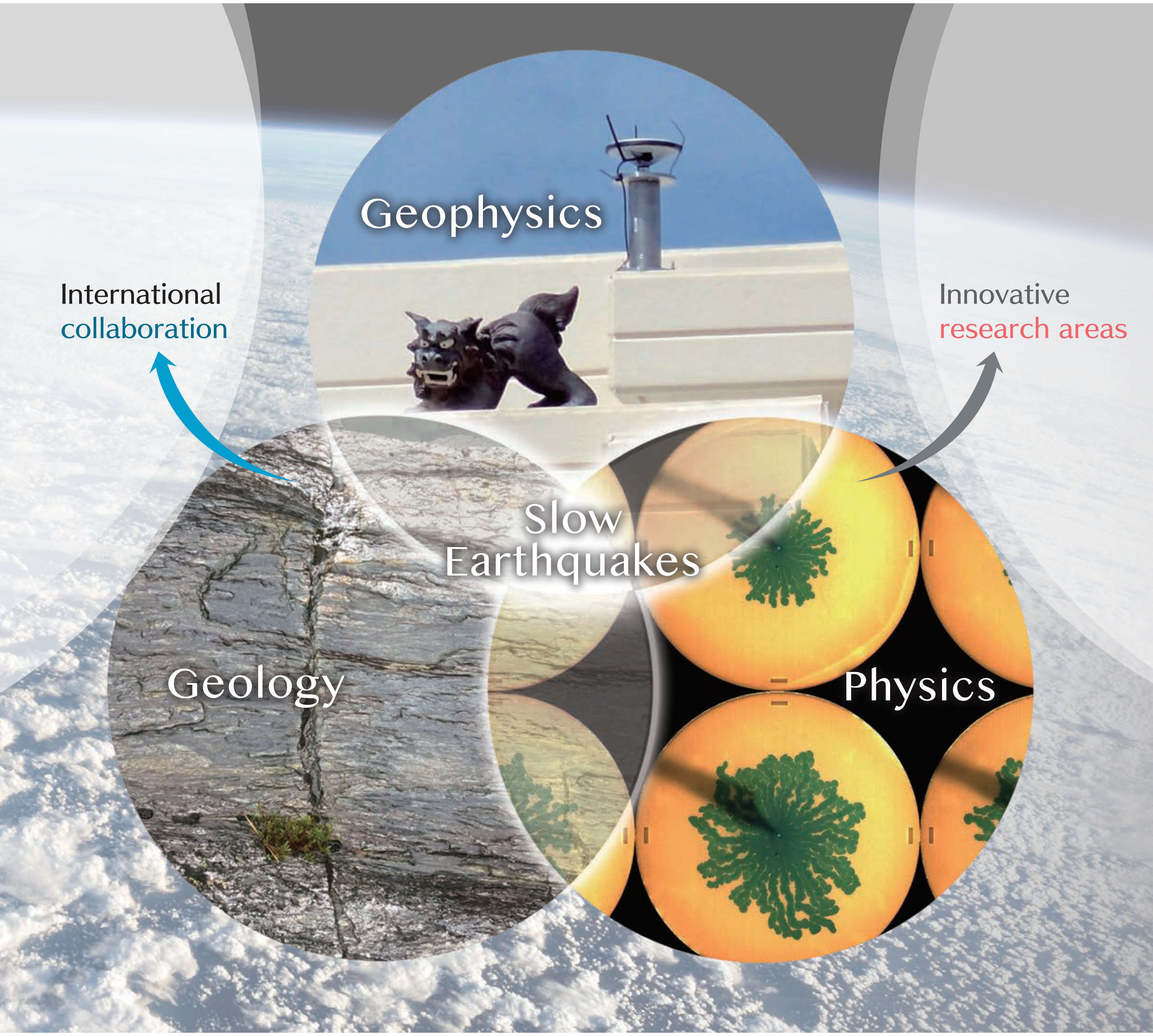

2016–2020 Japan Society for the Promotion of Science
Grant-in-Aid for Scientific Research
on Innovative Areas (JSPS KAKENHI No.2804)

INDEX

Introduction to Research in Group A01

Identification of possibly missing very low-frequency earthquakes

Masatoshi MIYAZAWA, Disaster Prevention Research Institute, Kyoto University

Various types of slow event, from low-frequency earthquakes or tremors to slow slips, are known to occur sometimes as a result of external perturbations. For example, low-frequency tremors can be activated by nearby earthquakes (Obara, 2002), and have also been triggered in phase and correlated with passing waves from large, distant earthquakes (Miyazawa and Mori, 2006). The latter is one of the few situations where a measurable stress can be identified as the immediate cause of low-frequency tremor, which helps us to understand the mechanism of its occurrence.

However, it is unclear whether immediate triggering of a very low-frequency earthquake, one of several types of slow earthquake, can occur by seismic waves. If this were the case, then investigation of this triggering may help to better understand the mechanisms of occurrence, as has been achieved for triggering of low-frequency tremor. Although there are a few cases of activation of very low-frequency earthquakes by passing waves (To *et al.*, 2015), identification of very low-frequency earthquakes during the passage of surface waves is difficult.

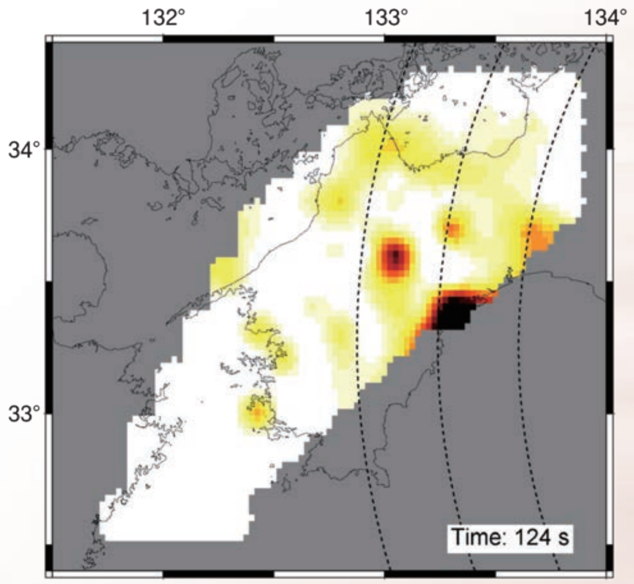

Fig. 1.
Log-likelihood distribution at 124 s after the 2016 off-Mie earthquake. Darker colors indicate a higher likelihood of occurrence of a very low-frequency earthquake. Dotted black curves are approximate arrivals of the large-amplitude waves shown in Figure 2.

Why is it difficult to identify immediate triggering of very low-frequency earthquakes? Both the amplitudes of low-frequency tremor and very low-frequency earthquakes are a few orders of magnitude smaller than that of the surface waves that are sufficiently large for triggering. In the case of the immediate triggering of low-frequency tremor (with a period of <1 s), the triggered events can be easily discovered by a simple signal processing that removes triggering surface waves with a period of about 20 s. However, this is not applicable to very low-frequency earthquakes because such earthquakes and surface waves have a similar predominant frequency. The same signal processing to remove surface waves as that applied for the detection of low-frequency earthquakes also removes the very low-frequency earthquake of interest. Therefore, to date, there has been no discovery of immediate triggering of very low-frequency earthquakes.

An attempt was made to detect signals from a possibly missing very low-frequency earthquake in the records of triggering waves (Miyazawa, 2019). A borehole array was used because comparing surface and borehole records can identify vertically incident body waves based on depth-dependent phase differences, which do not appear in records of horizontally propagating surface waves. These characteristics can be utilized for seismic data acquired by the KiK-net in Japan, a unique borehole seismic network. As the amplitude of very low-frequency earthquakes is expected to be very small, a stochastic approach was used for detection. Assuming that a triggered very low-frequency earthquake may exist, a particle filter method for waveform prediction was combined with a Markov chain Monte Carlo method for parameter estimation in terms of log-likelihood. In other words, this method finds the origin time and location of a very low-frequency earthquake that best explains the observed waveforms by trial and error, using a super-computer.

This approach was applied to seismic data in western Shikoku that recorded the 1 April 2016 Mw5.9 off-Mie earthquake (Miyazawa, 2019). The resolution of very low-frequency earthquake signals is limited

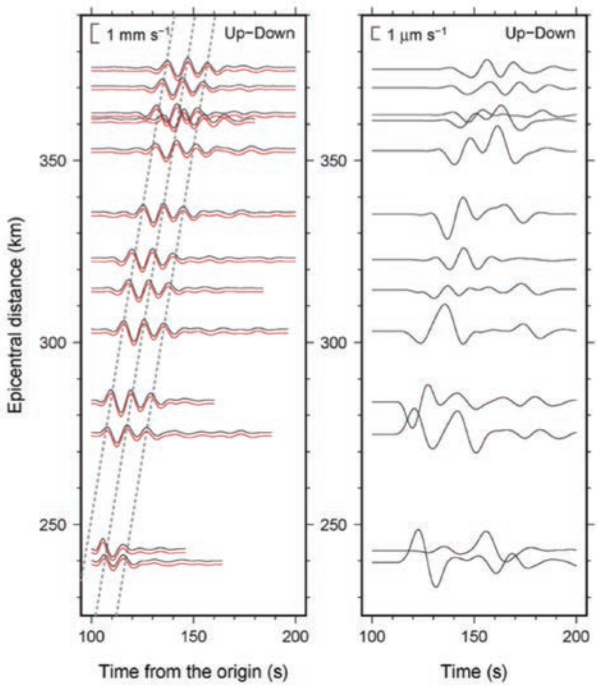

Fig. 2.
(Left) Observed waveforms of the 2016 off-Mie earthquake with respect to epicentral distance. Black represents the surface record and red represents the borehole record. (Right) Waveforms of detected very low-frequency earthquakes. Note that the amplitude scales of the waveforms of the left and right diagrams differ by three orders of magnitude.

because of the sensor specification, but at least six events with Mw~4 were likely triggered at the detection level during the passage of surface waves. It is noted that the magnitude may be poorly estimated. **Figure 1**, as an example, presents a snapshot of log-likelihood distributions after the off-Mie earthquake, which shows the locations where very low-frequency earthquakes likely occurred. The waveforms of the detected very low-frequency earthquakes are three orders of magnitude smaller than the off-Mie earthquake (**Fig. 2**). This is the first study to show that very low-frequency earthquakes can be immediately triggered dynamically, as other slow earthquakes are. This new discovery should provide insights into the mechanism(s) of occurrence of very low-frequency earthquakes.

References

Miyazawa, M. (2019), *J. Geophys. Intl*. 217, 1123–1140, doi:10.1093/gji/ggz073.

Miyazawa, M., and Mori, J. (2006), *Geophys. Res. Lett.* 33, L05303, doi:10.1029/2005GL025087.

Obara, K. (2002), *Science* 296, 1679–1681, doi:10.1126/science.1070378.

To, A., *et al.* (2015), *PEPI* 245, 40-51, doi:10.1016/j.pepi.2015.04.007.

Introduction to Research in Group A02

Long-term variation in the activity of short-term slow-slip events

Hitoshi HIROSE, Research Center for Urban Safety and Security, Kobe University

On the downdip extension of the megathrust earthquakes source area along the Nankai trough, so-called episodic tremor and slip (ETS), in which tremor coincides with a slow slip event, occurs frequently (Rogers and Dragert, 2003; Obara *et al*., 2004). As the locations of ETS sources are close to the megathrust zone, the ETS activity works as a stress buildup process on the megathrust zone, and the ETS and the megathrust earthquake cycle appear to be closely related (e.g., Obara and Kato, 2016). Because the macroscopic activity of an ETS episode is thought to be controlled by an SSE, which is much larger in spatial dimension than tremor, examination of the location and area of SSE slip regions, the size of SSEs, and their recurrence interval will help to understand the behaviors of ETS. It should be noted that an SSE that constitutes an ETS is referred to as a “short-term SSE” because its duration is relatively short; i.e., about a couple of days to weeks.

In southwestern Japan, short-term SSEs have been observed with tiltmeters (Obara *et al*., 2004), strainmeters (Kobayashi *et al*., 2006), and GNSS (Global Navigation Satellite System; Nishimura *et al*., 2013). Their fault motions have generally been modeled as a rectangular fault with uniform slip (i.e., the amount of slip does not depend on the location on the fault). Although this treatment is simple and useful for describing the approximate location and size of an SSE, the assumption may lead to a bias in defining the extent of an SSE slip area. Hirose and Obara (2010) estimated time-dependent slip evolutions for several short-term SSEs in the western Shikoku region, but did not estimate the slip distributions of all of the SSEs for the major ETS episodes, partly because of disturbances in the tilt time-series data.

To obtain as many slip distributions of short-term SSEs as possible, we applied a conventional inversion method to the tilt offset dataset that has been used for estimating rectangular fault models of SSEs in southwestern Japan produced by the National Research

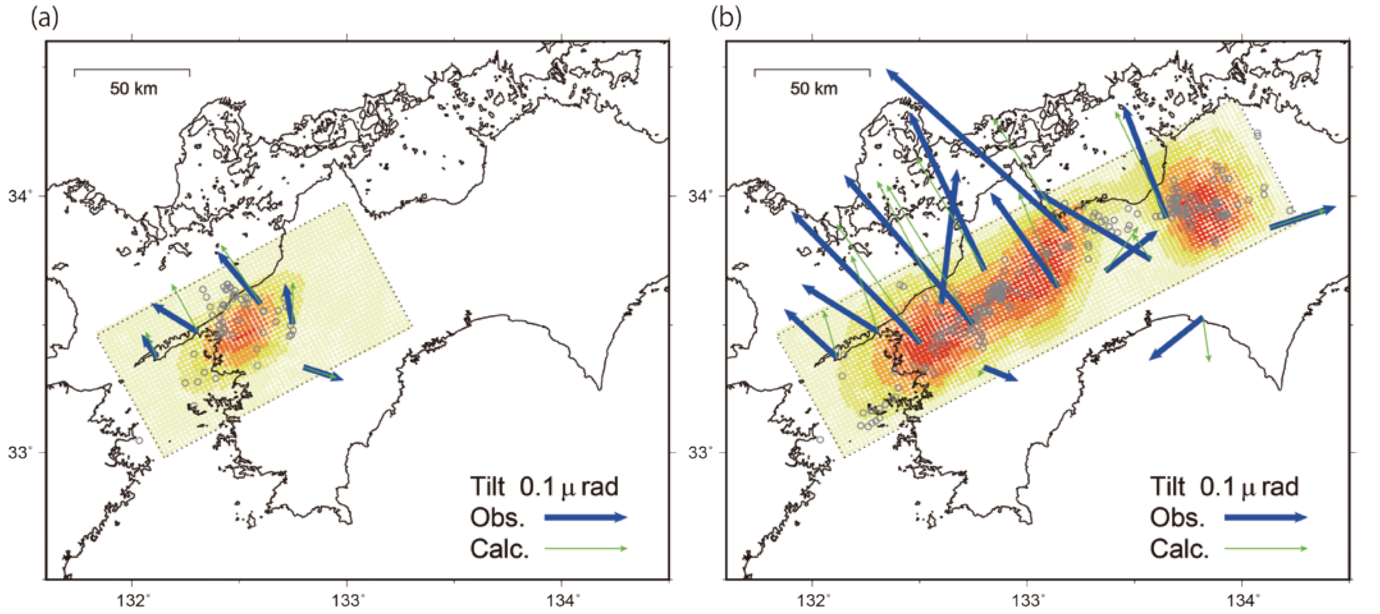

Fig. 1.
Slip distributions of short-term SSEs in Shikoku. The amount of slip at each position on the subducting plate interface is color coded and projected onto the surface. (a) April 2006 SSE; (b) February 2018 SSE. Blue arrows denote observed tilt change vectors, and green arrows show calculated tilt change vectors. Gray circles indicate tremor epicenters that occurred during each SSE (modified after Hirose and Kimura, 2020).

Institute for Earth Science and Disaster Resilience. We then obtained slip distributions for 61 short-term SSEs in Shikoku, which constitute all of the events for which rectangular fault models have been estimated over the past 18 years (Hirose and Kimura, 2020).

Figure 1 shows two examples of the estimated slip distributions. Slip is concentrated in a relatively small area for the April 2006 SSE (**Fig. 1a**) and is distributed over almost all of the ETS zone in Shikoku for the February 2018 SSE (**Fig. 1b**). The cumulative slip distribution for the past 18 years is spatially non-uniform, but there are three major segments in terms of slip activity of the short-term SSEs.

To examine the long-term variation in the extent of slip, the slip area of the SSEs in the strike direction is plotted as a function of SSE origin time in **Figure 2**. The number of SSEs that have larger slip extent seems to increase after 2012. Exploring what causes such a change in size of the SSEs should deepen our understanding, not only of the generation mechanism of slow earthquakes but also the preparation process of huge earthquakes.

References

Hirose, H., and Obara, K. (2010), *J. Geophys. Res.* 115, doi:10.1029/2008JB006050.

Hirose, H., and Kimura, T. (2020), *J. Geophys. Res.* 125, doi:10.1029/2020JB019601.

Kobayashi, A., *et al.* (2006), *Zisin* 2, 59, 19–27, doi:10.4294/zisin.59.19 (in Japanese).

Nishimura, T., *et al.* (2013), *J. Geophys. Res.* 118, doi:10.1002/jgrb.50222.

Obara, K., *et al.* (2004), *Geophys. Res. Lett.* 31, doi:10.1029/2004GL020848.

Obara, K., and Kato, A. (2016), *Science* 353, 253–257, doi:10.1126/science.aaf1512.

Rogers, G., and Dragert, H. (2003), *Science* 300, 1942–1943, doi:10.1126/science.1084783.

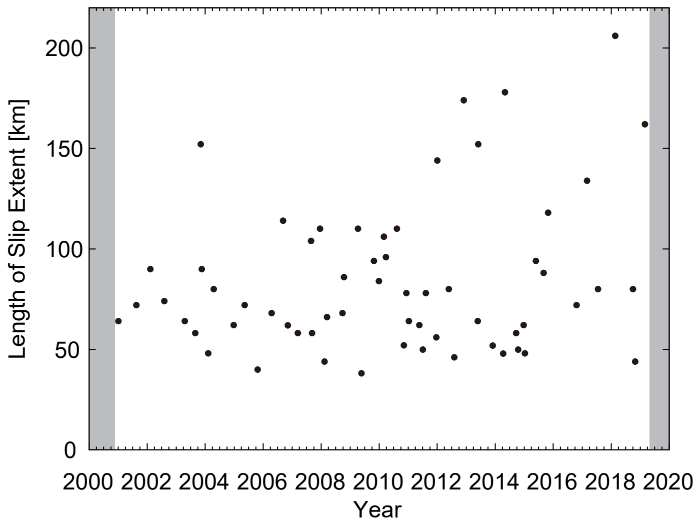

Fig. 2.
Length of slip extent of short-term SSEs versus time. Time periods with gray shading indicate those that were not analyzed.

Introduction to Research in Group B01

Heterogeneous structure in and around a slow-earthquake source region as revealed by an active source seismic experiment

Eiji KURASHIMO, Earthquake Research Institute, The University of Tokyo

The Nankai trough region, where the Philippine Sea Plate (PHS) subducts beneath the SW Japan arc, is a well-known seismogenic zone of interplate earthquakes. In recent years, slow earthquakes, which have various slip motions with different time-scales, have been recognized in regions adjacent to the seismogenic zone (e.g., Obara and Kato, 2016). A zone of nonvolcanic tremor has been found in the SW Japan fore-arc (Obara, 2002). Short-term slow-slip events (S-SSEs), which have durations in the order of days to weeks, have been detected along the Nankai Trough of SW Japan using GNSS data (e.g., Nishimura *et al*., 2013). Revealing the structural factors that control fault slip behavior is important for understanding subduction dynamics. The fluid pressure on a plate interface is one of the key factors on fault slip behavior (e.g., Saffer and Tobin, 2011). Seismic reflection characteristics can provide important information on the fluid-related heterogeneity of structures around the plate interface. To investigate the lateral variation in reflection characteristics along the low-frequency earthquake (LFE) zone, we conducted an active seismic experiment in the western part of Shikoku across the LFE zone in November 2019 (**Fig. 1**).

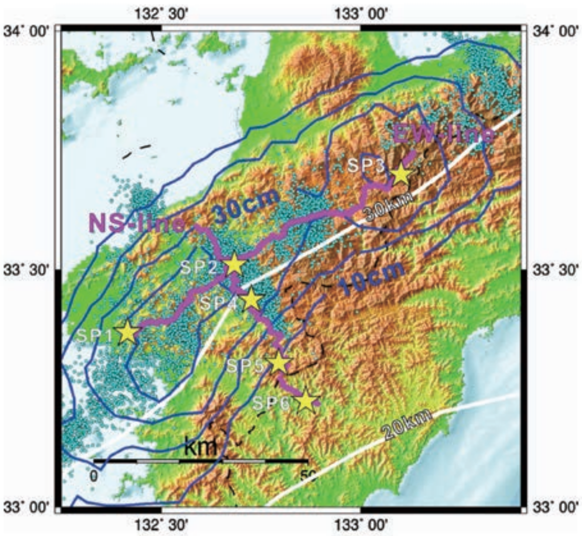

Fig. 1.
Seismic survey lines in the western part of Shikoku. Purple lines indicate active seismic survey lines. Yellow stars indicate shot-points. Blue circles indicate the epicentral LFE distribution determined by the Japan Meteorological Agency (1 April 2006 to 31 March 2016). Blue contour lines indicate the total cumulative slip of short-term SSEs (June 1996 to January 2012) (Nishimura *et al*., 2013). White contour lines indicate the depth to the upper boundary of the Philippine Sea Plate (Hirose *et al*., 2008).

Our seismic experiment was conducted along two survey lines. One was an 80-km-long seismic line between Seiyo and Kumakogen (E–W line) in the east–west direction and the other was a 50-km-long seismic line between Ozu and Shimanto (N–S line) in the north–south direction. A total of 600 seismic stations were deployed with ~200 m spacing for the E–W line and ~250 m spacing for the N–S line. Six explosive shots with a charge size of 200 kg were fired on the survey lines. We obtained high signal-to-noise ratio explosion data along the entire length of the profiles. The most remarkable feature of the record sections is that high-amplitude reflections, probably from the top of the subducting PHS, are recognized.

To obtain the reflection image, we applied a seismic reflection technique to the explosion data. The imaging was performed using conventional common mid-point processing steps, including post-stack migration and depth conversion. The normal moveout velocity and depth conversion velocity was based on a 3D velocity model (Matsubara and Obara, 2011). Seismic reflection images show several features of the deeper part of the hanging wall and the northward-dipping reflector interpreted as the top of the PHS at a depth range of 25–33 km (**Fig. 2**). Both downdip and along-strike variations in the reflection characteristics of plate boundary are recognized. Two large S-SSE slip areas (>40 cm; Nishimura *et al*., 2013) recognized on the E–W line (areas between SP1 and SP2 and near SP3) correspond to bright reflective zones. There is an apparent correspondence between changes in the reflection characteristics and changes in the slip distribution. Our results suggest that heterogeneous structure around the plate boundary may affect fault slip behavior.

References

Hirose, F., *et al*. (2008), *J. Geophys. Res*. 113, B09315, doi:10.1029/2007JB005274.

Nishimura,T., *et al*. (2013), *J. Geophys. Res*. 118, 3112–3125, doi:10.1002/jgrb.50222.

Matsubara, M., and Obara, K. (2011), *Earth Planets Space* 63, 663–667, doi:10.5047/eps.2011.05.018.

Obara, K. (2002), *Science* 296, 1679–1681, doi:10.1126/science.1070378.

Obara, K., and Kato, A. (2016), *Science* 353, 253–257, doi:10.1126/science.aaf1512.

Saffer, D. M., and Tobin, H. J. (2011), *Annu. Rev. Earth Planet. Sci*. 39(1), 157–186, doi:10.1146/annurev-earth-040610-133408.

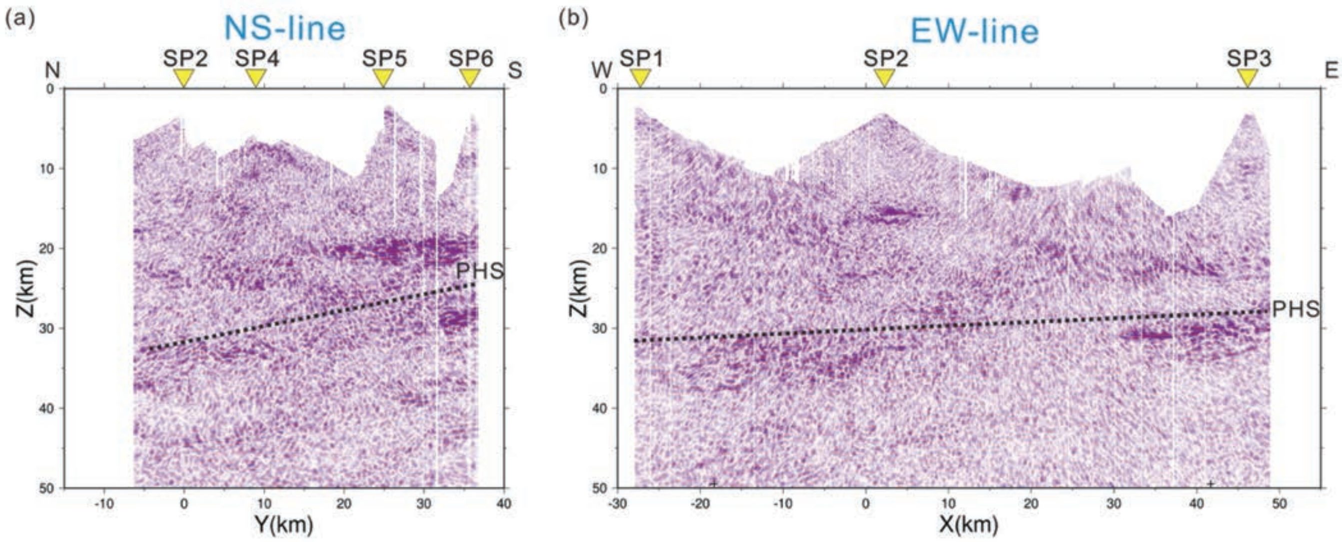

Fig. 2.
Post-stack migrated depth section with shot positions denoted by inverted yellow triangles. Dashed lines indicate our interpretation of the top of the PHS. (a) N—S line. (b) E—W line.

Introduction to Research in Group B02

Spatial relationships between stress caused by the geometry of decollement, material physical properties, and very low-frequency earthquakes

Yoshitaka HASHIMOTO, Kochi University

Slow earthquakes have been observed even at shallow subduction plate interfaces. It has been proposed that a heterogeneous distribution of rheological properties could control the occurrence of slip (Ando *et al.*, 2010). Such heterogeneous rheology could be related to material physical properties or stress (Fagereng and Sibson, 2010; Barnes *et al.*, 2020). Sun *et al.* (2020) presented a 2D model in which the relief on the plate interface, including seamounts, controls the distribution of stress and also the distribution of physical properties of sediments reacting to the stress.

The geometry and elastic velocity of shallow decollement in Nankai Trough off Kii Peninsula are available from detailed 3D seismic surveys (Moore *et al.*, 2007; Shiraishi *et al.*, 2020). In addition, slow slip events (SSEs) and very low frequency earthquakes (VLFEs) have been observed in the same area (Araki *et al.*, 2017; Nakano *et al.*, 2018). In this study, the spatial relationships between stress controlled by the decollement geometry, material physical properties inferred from velocity, and the occurrence of VLFEs are examined, followed by a discussion of the physical interactions between them.

Reflectors of the shallow decollement were traced from profiles in the 3D seismic box to produce the 3D geometry of the decollement. The dip azimuth and dip angle for 50 m × 50 m meshed surfaces on the decollement were calculated. A fault inversion method was adopted for the lower-angle nodal plane and the slip direction from CMT mechanisms of the VLFEs to estimate the regional stress. The regional stress indicates NW—SE horizontal compression with a stress ratio of 0.65 (difference between the intermediate and minimum stresses normalized by the differential stress). Combining the regional stress and the directions of the meshed surfaces, normal and shear stresses on the meshed surfaces were calculated notionally using the stress ratio and a frictional coefficient for the decollement. Slip tendency (Ts) is defined by the ratio of shear stress to normal stress. The surface slips easily with a large Ts. Dilation tendency (Td) is defined by the difference between the normal stress and the maximum principal stress normalized by the differential stress. The surface opens easily with a large Td. We obtained the distributions of Ts and Td on the meshed surfaces of the shallow decollement (**Fig. 1**). The distribution of Ts shows weakly continuous NE—SW trends with large and small values repeated in the depth direction. The distribution of Td is the same as that of Ts, and the pattern of large and small values of Td is consistent with that of Ts. In addition, very small Ts and Td values are distributed,

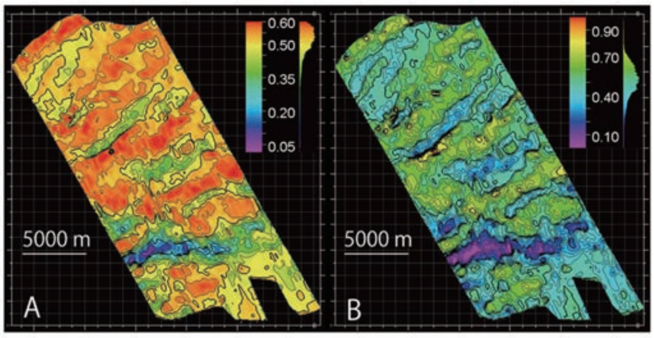

Fig. 1.
Distributions of Ts and Td in the shallow decollement.

trending E−W in the very shallow portion (**Fig. 1**).

The averaged elastic velocity within the interval between 100 m above and below the decollement was obtained to estimate the physical properties of sediments. The velocity shows a general increase with depth, and the areas with relatively fast or slow velocities trend in the NE−SW direction. The effective pressure and porosity are estimated at 3500−6000 kPa and 5%−20%, respectively, as calculated by a conversion from velocity using relationships between velocity, effective pressure, and porosity from laboratory experiments (Hashimoto and Yamaguchi, 2014).

We also examined the spatial relationship between the distributions of Ts, Td, and VLFEs. VLFEs migrated from deep to shallow regions during the 18 days from 1 April 2016. VLFEs are aligned NE−SW for specific time windows (**Fig. 2**). The trend of the aligned VLFEs is parallel to the trends of Ts and Td. The area with very small Ts and Td seems to act as a barrier to the migration of VLFEs (**Fig. 2**). VLFEs were more likely to occur in the area of large Ts values. This area also has large Td values, which suggests that it may be a conduit for fluid flow during the seismic events.

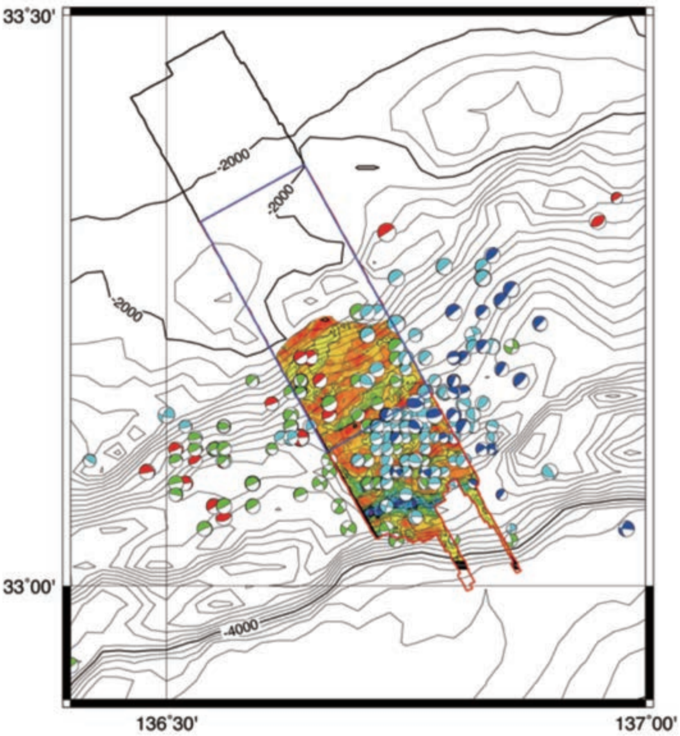

Fig. 2.
Spatial relationship between the distributions of Ts and VLFEs. Colors of CMT solutions show time windows of events.

The distributions of Ts and Td are also parallel to the distribution of sediment material properties, although the areas with large and small values of Ts and material properties are not completely consistent. Although the reason for the inconsistency between values of Ts and sediment properties needs to be examined in the near future, the parallel distribution relationship between them suggests that Ts and Td exert at least some influence on these properties.

Our results suggest that the stress distributions caused by decollement geometry and regional stress have strong relationships with the distribution of VLFEs and with sediment material properties. These relationships suggest that decollement geometry can be a primary control on the other variables, as Ts and Td are calculated only from decollement geometry and regional stress. Because Ts and Td have a strong spatial relationship to both VLFEs and sediment material properties, it is inferred that the geometry and regional stress likely control VLFE activity and material properties.

Similarly, in Hyuga-Nada, where the Kyushu-Palau ridge subducts, shallow tremor and VLFEs are distributed around a subducting seamount (Yamashita *et al*., 2015). A new drilling program has been proposed for the International Ocean Discovery Program (IODP) to understand the effects of the subducting seamount on VLFE activity.

References

Ando, R., *et al.* (2010), *Geophys. Res. Lett.* 37, doi:10.1029/2010GL043056.

Araki, E., *et al.* (2017), *Science* 356, 1157–1160, doi:10.1126/science.aan3120.

Barnes, P. M., *et al.* (2020), *Science Advances* 6, eaay3314, doi:10.1126/sciadv.aay3314.

Fagereng, A., and Sibson, R. H. (2010), *Geology* 38, 751–754, doi:10.1130/G30868.1.

Hashimoto, Y., and Yamaguchi, M. (2014), *Proc. IODP* 333, doi:10.2204/iodp.proc.333.202.2014.

Moore, G., *et al.* (2007), *Science* 318, 1128-1131, doi:10.1126/science.1147195.

Nakano, M., *et al.* (2018), *Nature communications* 9, 984, doi:10.1038/s41467-018-03431-5.

Shiraishi, K., *et al*. (2020), *Earth, Planets and Space* 72, 1–14, https://doi.org/10.1186/s40623-020-01204-3.

Sun, T., *et al.* (2020), *Nature Geoscience* 13, 249–255, https://doi.org/10.1038/s41561-020-0542-0.

Yamashita, Y., *et al.* (2015), *Science* 348 (6235), 676–679, doi:10.1126/science.aaa4242.

Introduction to Research in Group C01

Forecasting crustal deformation using machine learning

Yuta MITSUI, Faculty of Science, Shizuoka University

Machine learning is a generic term for algorithms that build statistical models autonomously based on sample data (termed "training data") and has been rapidly adopted in seismology-related fields. Specific examples include picking P-wave arrivals (Ross *et al.*, 2018), identifying earthquake and tremor signals from spectrograms (Nakano *et al.*, 2019), detecting a nucleation phase of slow slip events (Hulbert *et al.*, 2020), predicting aftershock distribution (DeVries *et al.*, 2018), and accelerating viscoelastic calculations (DeVries *et al.*, 2017). The estimation of block boundaries by clustering surface velocities, such as that performed by Savage (2018) for the entire Nankai Trough, is also a form of machine learning.

We focused on recurrent neural networks (RNNs) among various machine learning algorithms. RNNs are suitable for analyzing time-series data. The resultant models are trained by comparing outputs from previous sequences with the next values, as shown in **Figure 1**.

Yamaga and Mitsui (2019) selected the postseismic deformation of the 2011 Tohoku earthquake as a "data-rich" and "good signal-to-noise ratio" event, for a trial of crustal deformation forecast using RNN. We used the F3 solution of GEONET, a GNSS observation network managed by the Geospatial Information Authority of Japan. Nishimura (2014), Tobita (2016), Morikami and Mitsui (2020), and others have conducted regression analyses of this event, which can be used as a comparator for RNN forecasts.

Our model was trained with time-series data from 153 stations in northeastern Japan, and we carried out forecast experiments at another 38 stations. In the experiments, time-series data for one year after the mainshock were used, and the subsequent changes in the postseismic deformation were forecasted and compared with the observed data.

We found that, for a period of about seven years after the mainshock, the forecasts were more accurate than regression analyses without falling into over-learning. We obtained other results by focusing on the spatio-temporal evolution of the difference between

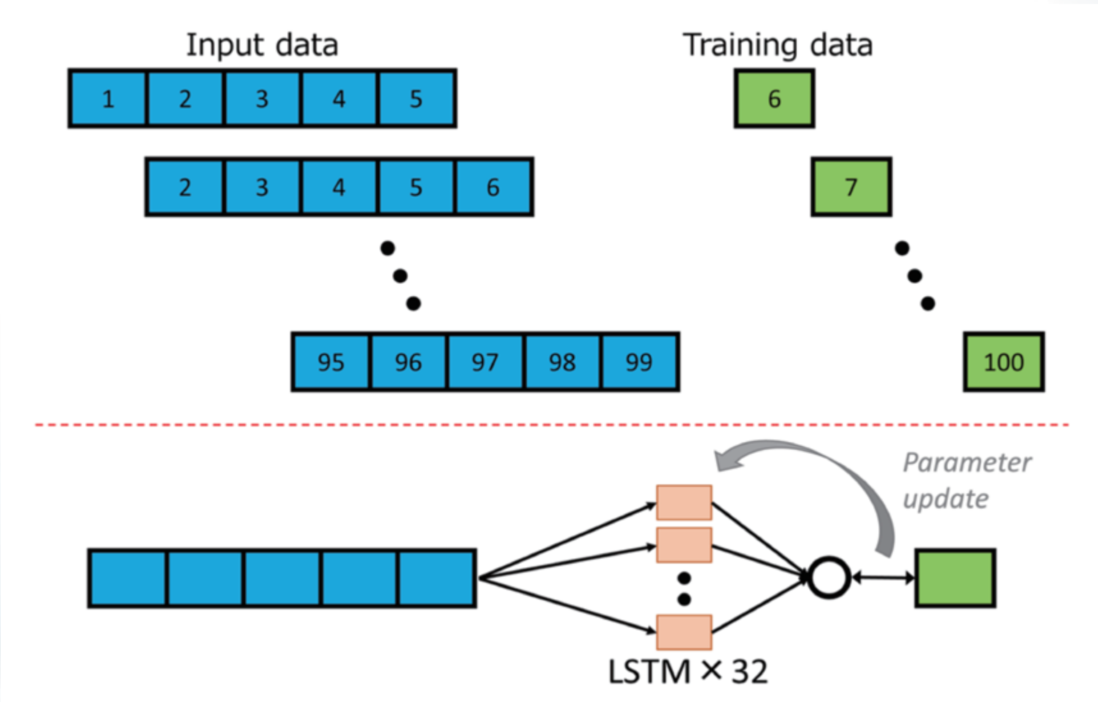

Fig. 1.
Conceptual diagram of a recurrent neural network (RNN). In this study, we set up long short-term memory (LSTM) units for long-term memory.

the forecast results and the observed data, which may reflect physical mechanisms. More information is contained in the study of Yamaga and Mitsui (2019).

Currently, the work is still in the exploratory stage, and the exact nature of the scientific progress that the study will make will become clearer in the near future.

References

DeVries, P. M. R., *et al*. (2018), *Nature* 560, 632–634, doi:10.1038/s41586-018-0438-y.

DeVries, P. M. R., *et al*. (2017), *Geophys. Res. Lett*. 44, 2662–2669, doi:10.1002/2017GL072716.

Hulbert, C., *et al*. (2020), *Nat. Comm*. 11:4139, doi:10.1038/s41467-020-17754-9.

Morikami, S., and Mitsui, Y. (2020), *Earth Planets Space* 72:37, doi:10.1186/s40623-020-01162-w.

Nakano, M., *et al*. (2019), *Seis. Res. Lett*. 90, 530–538, doi:10.1785/0220180279.

Nishimura, T. (2014), *J. Dis. Res.* 9:3, doi:10.20965/jdr.2014.p0294.

Ross, Z. E., *et al*. (2018), *J. Geophys. Res.* 123, 5120–5129, doi:10.1029/2017JB015251.

Savage, J. C. (2018), *J. Geophys. Res.* 123, 1954–1968, doi:10.1002/2017JB014874.

Tobita, M. (2016), *Earth Planets Space* 68:41, doi:10.1186/s40623-016-0422-4.

Yamaga, N., and Mitsui, Y. (2019), *Geophys. Res. Lett.* 46, 11886–11892, doi:10.1029/2019GL084578.

Introduction to Research in Group C02

Analog Experiments for Slow Earthquakes — Toward Controlling Frictional Behavior —

Tetsuo YAMAGUCHI, Department of Biomaterial Sciences, The University of Tokyo

It is well known that fast frictional slip in regular earthquakes is driven by the release of stored elastic energies, and seismic waves are consequently radiated. In contrast, slow slip and almost no seismic waves are generated for slow earthquakes. A question arises as to what controls fast slip and radiation of seismic waves in slow earthquakes? At present, several phenomenological explanations have been given, including a reduction in weakening due to a decrease in effective normal stress, the existence of viscous fault zones surrounding brittle patches, and the localization of slip zones.

The following question comes next: what are the origins of slow earthquakes in terms of materials? There have been intensive geological studies in this project and some promising mechanisms have been proposed. In near future, clearer and more definite scenarios will be made.

Through these kinds of discussion, a question arises to me: is it possible to perform experiments which demonstrates slow earthquakes? Such a question motivated me to start laboratory experiments using analog materials in a simple setup.

First, we pulled a gel sheet over a glass substrate,

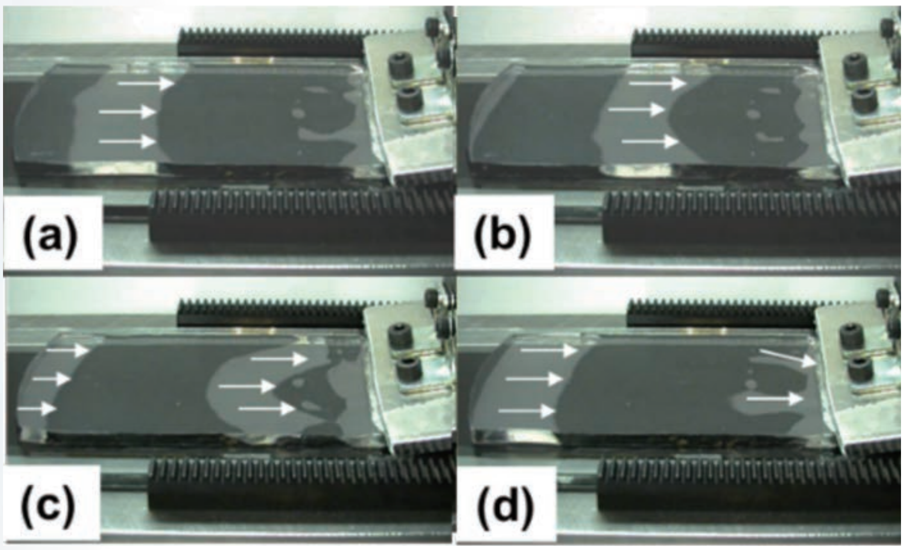

Fig. 1.
Slow propagation of slip pulses. (T. Yamaguchi *et al*, 2009)

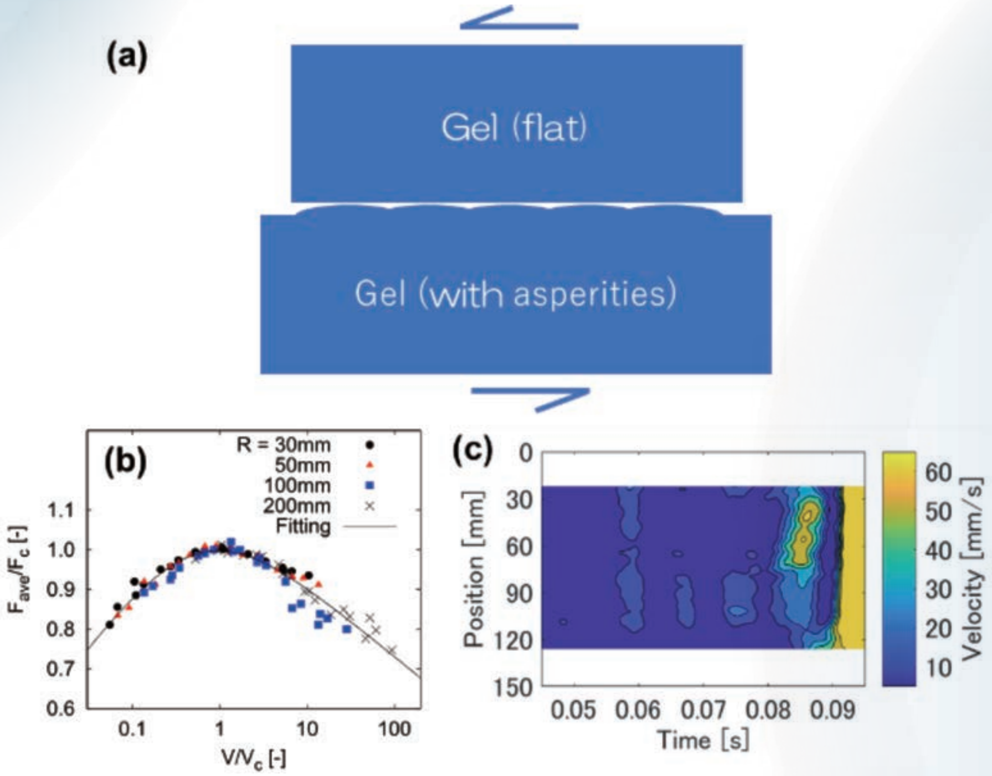

Fig. 2.
(a) Experimental setup, (b) frictional constitutive behavior, and (c) spatio-temporal map of slip velocities. (Fukudome *et al*., in preparation)

as shown in **Figure 1**. With this setup, we were able to observe slow propagation of slip pluses (V_{pulse} ~ mm/s, about 1000 times smaller than V_S). The mechanisms for slow propagation can be explained in terms of two characteristics. The first is the thin plate geometry of the gel; as the region of elastic energy storage is limited, the rupture propagation does not reach the terminal velocity. The second is the high resistance to crack propagation caused by the high viscosity of the gel.

Although this simple experiment appeared to be successful in reproducing slow slip, the huge contrast in elasticity (G_{gel} is 10^6 times smaller than G_{glass}) causes a mismatch in elastic deformation and separation of the gel from the glass, leading to weakening of the frictional interface. This is a general mechanism, as exemplified by the friction between an automobile tire and the road, but it does not occur on tectonic faults with huge static pressure. Accordingly, we examined friction experiments with similar materials, that is, between gel and gel. However, initially, such a combination did not work for the utilized gels. Despite our various efforts, such as the placement of asperities and the control of material properties and shape, no "earthquakes" were observed.

After struggles for several years, we were able to get a clue for a success; by placing thin asperities (with a large curvature radius) on the surface of the gel, we observed stick-slip motions. We then studied the effects of curvature radius of the asperities, normal stress, and sliding velocity on the frictional behavior, and established frictional constitutive laws with a non-monotonic rate dependence. Moreover, we identified tremor-like rupture behavior in the nucleation phase (**see Fig. 2**).

As described here, we have been to reproduce earthquakes in our laboratory setup. However, we have not yet been able to control the frictional properties (including friction constant, slope, critical velocity, and introduction of velocity-strengthening at higher velocities). Our experiences suggest difficulty in controlling friction, but we intend to pursue this goal during future study.

References

Yamaguchi, T., Ohmata, S., and Doi, M. (2009), *J. Phys: Condensed Matt.* 21, 205105, doi: 10.1088/0953-8984/21/20/205105.

Fukudome, T., Otsuki, M., Selvadurai, P. A., Sawae, Y., and Yamaguchi, T. in preparation.

Introduction to Publicly Offered Research in Group A01

Array observation of volcanic low-frequency earthquakes

Naofumi ASO, Tokyo Tech.

Low-frequency earthquakes are classified as either tectonic or volcanic type. As the physical mechanism of the volcanic type is poorly understood, I have been operating a small seismic array in Shobara, Hiroshima, to capture the seismicity and first motions of low-frequency earthquakes in Shimane and Tottori. I deployed four short-period seismometers on stable rocks every 100—200 m. I visit the site every other month to collect data and replace batteries in the offline stations.

These seismograms have higher S/N ratios than those of permanent stations. The stacking of four stations enhances clarity of the first motion. Using matched-filter analyses, I obtained a more complete seismicity catalog of the swarm-like activity that occurred on 29 March 2020. As such swarm-like activity is unique to volcanic low-frequency earthquakes, I further investigated the characteristics of this activity.

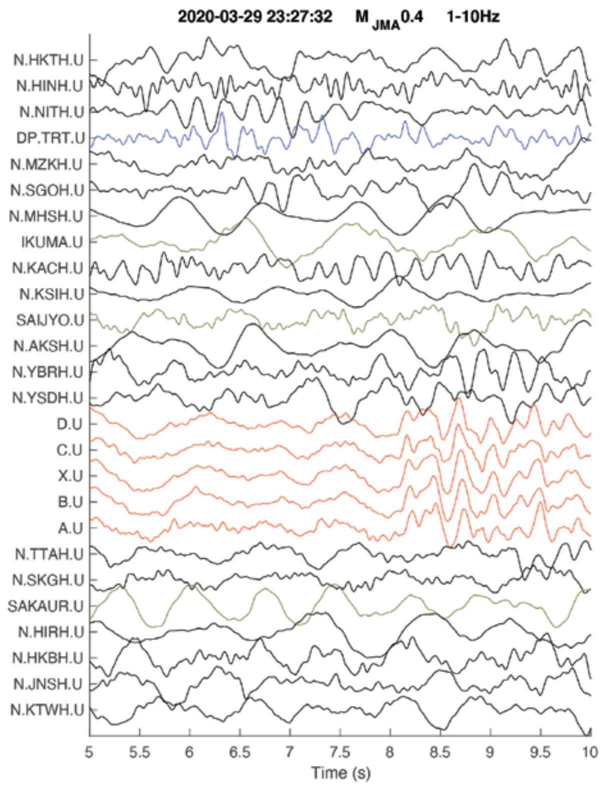

Fig. 1.
Observed seismograms (A—D) and their stacked waveform (X).

Introduction to Publicly Offered Research in Group A01

Characteristics of shallow very low-frequency earthquake activity along the Nankai Trough determined by incorporating the effects of a 3D heterogeneous structure model

Shunsuke TAKEMURA, ERI, UTokyo

Because of the effective propagation of long-period surface waves, shallow very low-frequency earthquakes (VLFEs) have been widely detected by the long-term (~15 years) onshore broadband network. We conducted CMT (Centroid Moment Tensor) inversion of shallow VLFEs based on a 3D Green's function dataset. Our CMT catalog reveals temporal activity patterns of shallow VLFEs along the Nankai Trough (**Fig. 1**). We also carried out a cross-correlation analysis to precisely locate shallow VLFE epicenters. The shallow VLFE distributions tend to cluster in or migrate into regions surrounding the plate boundary stress peaks. This result suggests that shallow slow earthquakes occur and migrate to release accumulated stress in transitional regions along the Philippine Sea plate boundary (**Fig. 2**).

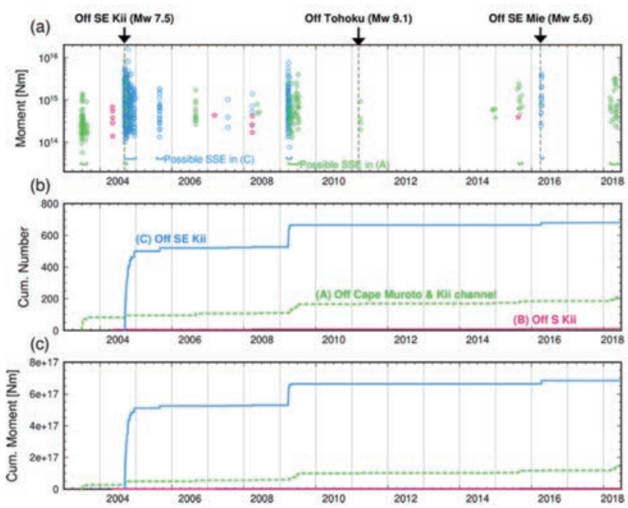

Fig. 1.
Temporal activity patterns of shallow VLFEs along the Nankai Trough.

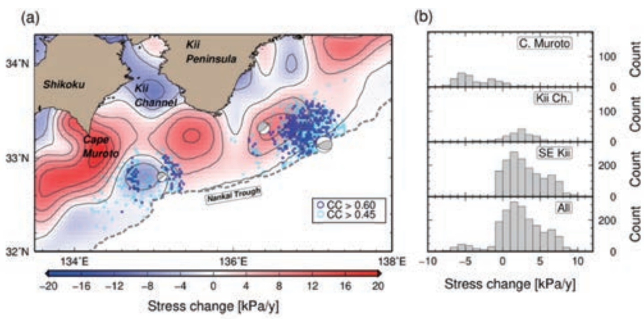

Fig. 2.
Spatial distributions of shallow VLFEs and shear stress change rate at the plate boundary (Noda *et al.*, 2018).

Introduction to Publicly Offered Research in Group A02

Episodic tremor and slip invades the strongly locked megathrust in the Nankai Trough

Masayuki KANO, Tohoku Univ.

Slow earthquakes often occur adjacent to seismogenic zones. Among the various types of slow earthquake, signals of short-term slow-slip events (S-SSEs) are frequently too small to detect by using GNSS (Global Navigation Satellite System) observations. We applied the method of Frank *et al*. (2015) to obtain cumulative crustal deformation caused by a series of S-SSEs by referencing the numbers of low-frequency earthquakes to GNSS data in southwest Japan, and extracted signals of a series of known SSEs and inferred slip distributions in detail. The extracted displacements due to 12 S-SSEs are oriented nearly opposite to the direction of plate subduction and have a maximum amplitude of ~1.5 cm (**left panel of Fig.1**). The inverted slip indicates two fault patches: a deeper one in the transition zone and a shallower one at a depth of ~20 km (**right panel of Fig.1**), which corresponds to the bottom of the large slip deficit zone and the coseismic slip area in the 1946 Nankai earthquake. This result indicates that the S-SSEs in the deeper patch in some cases excite the shallow slip transient at the bottom of the locked area, which can be explained by along-dip fluid migration.

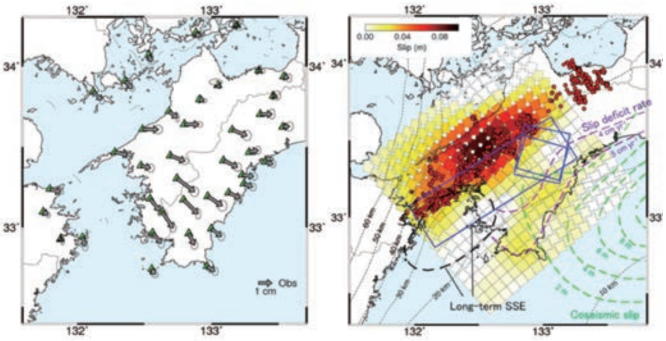

Fig. 1.
(Left) Cumulative crustal deformation resulting from 12 S-SSEs. (Right) Slip distribution. Purple and green lines indicate the contours of slip deficit rate and coseismic slip during the 1946 Nankai earthquake revealed by previous studies, respectively. (Figure from Kano *et al*., 2019)

Introduction to Publicly Offered Research in Group B01

Fault structure, seismic anisotropy, and a subducting seamount in the northern Hikurangi margin

Ryuta ARAI, JAMSTEC

To reveal the physical and frictional properties of the source regions of active slow earthquakes, a 3D anisotropic P-wave velocity structure model was constructed for the northern Hikurangi margin, New Zealand, where active slow earthquakes occur frequently in the shallow (<10 km depth) part of the plate boundary. To construct the model, travel time tomography analysis was applied to 3D seismic refraction data obtained during an international collaborative study by JAMSTEC. The model shows that the anisotropy is not ubiquitous and homogeneous within the overriding plate, and that significant (>5%) anisotropic features occur in the vicinity of active branching faults in the accretionary wedge and the deformation front (**Fig. 1**). These features suggest that not only preferentially oriented cracks, but also fault-bound clay-rich sedimentary layers, contribute to the production of upper-plate anisotropy. In addition, the subducting seamount is inferred to be located ~10 km further downdip than previously thought, and forms a subduction channel in its wake that consists of fluid-rich sedimentary and volcaniclastic rocks (**Fig. 2**). This process may facilitate fluid transport deep into the subduction zone.

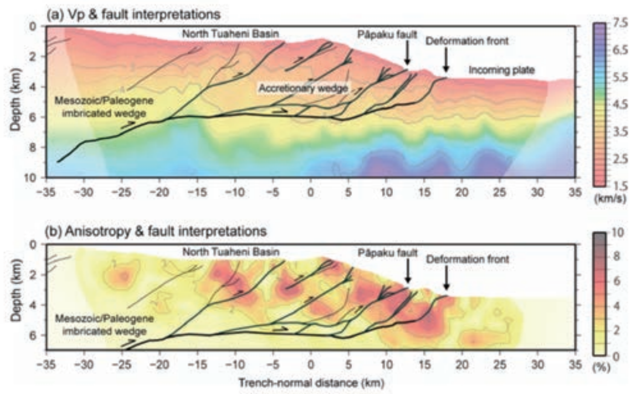

Fig. 1.
P-wave velocity and anisotropy structures in the northern Hikurangi margin (Arai *et al*., 2020).

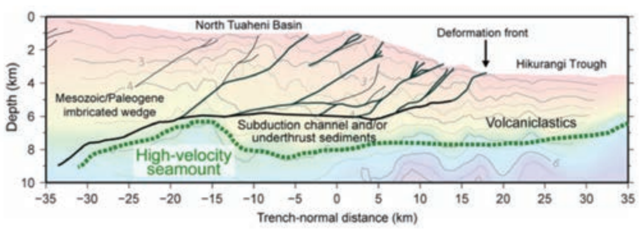

Fig. 2.
Structural model of seamount subduction in the northern Hikurangi margin (Arai *et al*., 2020).

Introduction to Publicly Offered Research in Group B01

Slow slip and intraslab earthquakes

Saeko KITA, BRI

In general, the timing of intra-slab earthquakes is related to that of slow slip, but the mechanism of this relationship is unknown. To examine the mechanism of the relationship between intra-slab earthquakes and slow slip, we investigated spatial and temporal variations in the subducting slab using the focal mechanisms and seismicity of intraslab earthquakes. We measured the change in the stress axis in the slab before and after the occurrence of episodic tremor and slip, and found that this change is larger near the trench axis than in the region where ETS occurs (**Fig. 1**). The peak b-values of intra-slab earthquakes occurred 1.5 months before ETS took place, which is consistent with the characteristics of seismicity caused by fluid injection. These results suggest that the migration of fluid from the slab into the plate boundary where slow earthquakes occur is the likely mechanism linking the occurrences of slow earthquakes and intra-slab earthquakes. Furthermore, monitoring the conditions of the slab itself could be useful for better understanding the state change of the plate boundary where a large subduction-zone earthquake will occur.

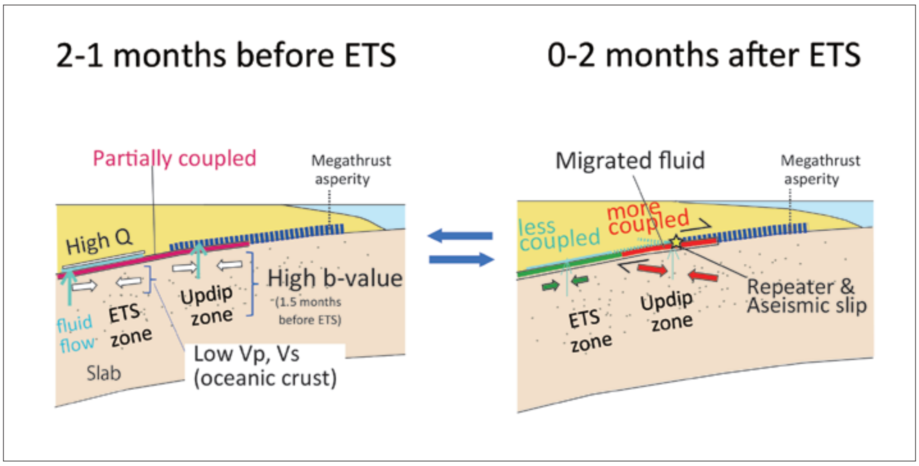

Fig. 1.
Schematic cross-sectional views beneath the Kii peninsula before and after the occurrence of ETSs.

Introduction to Publicly Offered Research in Group B01

Fluids and shallow slow earthquakes

Takashi TONEGAWA, JAMSTEC

We investigated the relationship between fluids and slow earthquakes in the shallow part of the Nankai subduction zone. We extracted Ps (P-to-s) reflections from the megasplay fault and another fault between it and the top of the oceanic crust, using P-waves radiated from ship noise of the drilling vessel Chikyu. Ps amplitudes were found to vary with tidal forces, which can be explained by fracture connection and isolation with fluids within the faults. Previously reported SSEs might have occurred along these multiple weak faults.

We also extracted surface waves from ambient noise records observed by DONET (Dense Oceanfloor Network system for Earthquake and Tsunami) and investigated the temporal variation in heterogeneous seismic structure. The heterogeneous structure may be changed by fluid migration, and this fluid migration is linked to slow earthquake generation. This finding should contribute to our understanding of the relationship between slow earthquake generation and fluid migration.

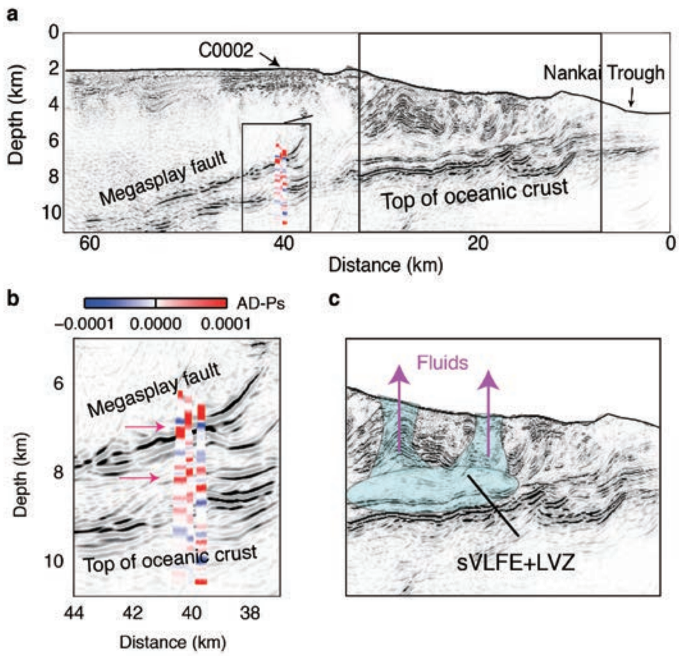

Fig. 1.
(a) Locations where velocity contrasts vary with tidal stress, plotted on a seismic image (Shiraishi *et al.*, 2019). (b, c) Zoomed domains of (a) with our interpretation.

Introduction to Publicly Offered Research in Group B02

Formation processes of quartz veins in the region of deep slow earthquakes

Asuka YAMAGUCHI, AORI, UTokyo

To obtain a better understanding of the relationships among deep slow earthquakes, rheology, fluid flow, and mineral precipitation along subduction plate interfaces, a geological investigation was made of on-land accretionary and metamorphic complexes. On the Kerama Islands, Okinawa, the first occurrence of mylonite in the Shimanto accretionary complex was discovered. Geochronological and paleothermal results reveal that the accretionary complex was formed at ~100 Ma, with a maximum temperature of ~500 °C. Changes in deformation mechanisms and the brittle–plastic transition are recorded in the rocks on the Kerama Islands, including a series of deformation episodes, dissolution–precipitation creep, and quartz-vein formation within pelitic rocks (Fig. 1). Plastic deformation in conglomerate-origin mylonite (Fig. 2) occurred during the subduction of extremely young oceanic plate immediately following ridge subduction. Field observations suggest that abundant quartz veins were formed just before subducted sediments passed through the brittle–plastic transition. It is expected that further analyses of the mylonite should constrain the rheology of the subduction plate interface.

Fig. 1.
Quartz veins in pelitic schist.

Fig. 2.
Conglomerate-origin mylonite.

Introduction to Publicly Offered Research in Group B02

Rheology of the fluid-oversaturated fault zone at the brittle–plastic transition

Keishi OKAZAKI, KCC/JAMSTEC

High Vp/Vs ratios are commonly observed in the source region of deep slow earthquakes. We conducted experiments to investigate the rheology of quartz, a dominant component of subducting sediments, with different fluid fractions at the high-pressure and high-temperature conditions that characterize the BPT. The strength of quartz aggregates with fluid fractions of 5–25 vol.% is significantly lower than that predicted by wet quartzite flow laws and decreases with increasing fluid fraction. Recovered samples deformed in the ductile regime exhibit S–C' mylonitic structures that are characterized by elongate grains, shear localization, and fluid segregation. Variations in strength are explained by a combination of a constitutive law for dislocation creep that includes the geometric effects of fluid fraction, a friction law that includes the effect of fluid fraction through its role on the real area of contact, and an empirical function to describe the smooth brittle–plastic transition. Our results indicate that the presence of fluid-filled porosity promotes significant weakening in shear zones and that variations in fluid fraction (together with temperature) can explain transitions in the spectrum of slip behaviors observed along plate boundaries.

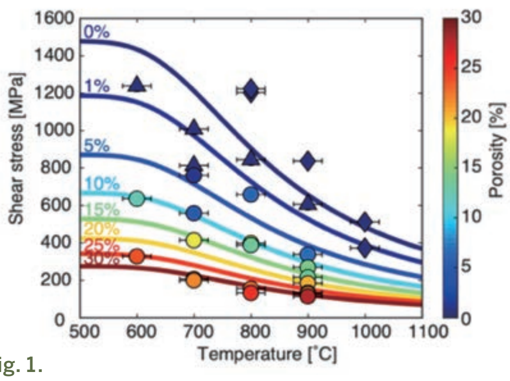

Fig. 1.
Shear stress versus temperature of fluid-oversaturated quartz aggregates. Thick lines indicate theoretical predictions with different fluid fractions (%).

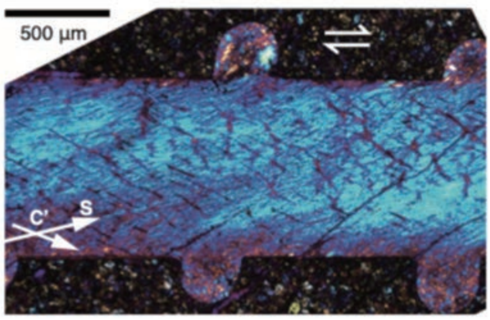

Fig. 2.
Image of the microstructure of the recovered sample, under cross-polarized light and a half-wave-length plate.

Introduction to Publicly Offered Research in Group B02

Slip acceleration to dynamic weakening in rock analogs

Miki TAKAHASHI, Geological Survey of Japan, AIST

Earthquake nucleation and propagation can be only partly comprehended without understanding the acceleration of slip on a fault. To elucidate the physics behind slip acceleration, rotary shear experiments were performed, involving step increases in shear stress on a brine-saturated, 80:20 (wt.%) mixture of halite and muscovite gouge under conditions of room temperature and 5 MPa normal stress. The resultant velocity-strengthening relationship is comparable with those found in previous studies (e.g., Niemeijer and Spiers, 2007, JGR; Takahashi *et al.*, 2017, G-cubed) that limit steady-state velocity to <1 μm/s (**Fig. 1**). For velocities exceeding 1 μm/s, however, runaway slip occurs, and dynamic weakening starts to appear at 20 μm/s. It is noted that the fault maintains shear stress at the maximum shear strength for several hours before the appearance of dynamic weakening, even though the steady-state strength decreases substantially. These two critical velocities are key to describing the dynamic behavior of fault slip. The delay in dynamic weakening can be explained by the direct effect that temporarily strengthens the simulated gouge. A previous study (Takahashi *et al.*, 2017) suggested that the direct effect has an abnormally high value (~0.1) at 1 μm/s, but is almost negligible at 20 μm/s. This means that the fault accelerates the slip, but still sustains the shear stress for velocities greater than the lower critical value, and promotes dynamic weakening at the higher value. Therefore, measurement of these key velocities in nature should substantially improve the understanding of earthquake nucleation and propagation processes.

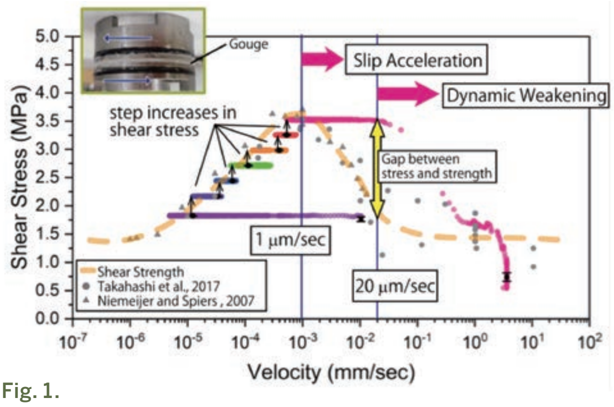

Fig. 1.
Evolution of slip velocity for step increases in shear stress (colored dots). The dashed yellow line depicts the approximate change in steady-state shear strength as a function of velocity, based on previous experimental results (gray symbols).

Introduction to Publicly Offered Research in Group B02

Direct evidence for mixed brittle and plastic deformation at high pore fluid pressures recorded in a paleo-mantle wedge serpentinite body

Ken-ichi HIRAUCHI, UShizuoka

In warm subduction zones such as those of Nankai and Cascadia, episodic tremor and slip (ETS) occurs at the base of the serpentinized forearc mantle wedge. To understand the relationship between serpentinite deformation and ETS generation, a mantle-wedge-derived serpentinite body was studied that formed at pressure (P)–temperature (T) conditions similar to those of the ETS source region (i.e., P = 1 GPa, T = 400 °C), in the Sanbagawa metamorphic belt, Shikoku, Japan. The serpentinite body exhibits block-in-matrix structures (**Fig. 1**) that resulted from the formation of extensional and extensional shear fractures at high pore fluid pressure (P_f). The opening of fractures results in a sudden drop in P_f and is sealed by a serpentine (antigorite) matrix (**Fig. 2**). The matrix antigorite that is aligned along some fractures is dynamically recrystallized via dislocation glide on the (001) plane, perhaps at relatively low P_f conditions (**Fig. 2**). The observed mutual crosscutting relationship between fracturing and dynamic recrystallization indicates multiple episodes of coeval brittle–plastic deformation caused by cyclic changes in P_f.

Fig. 1.
Outcrop photograph of serpentinite showing block-in-matrix structure.

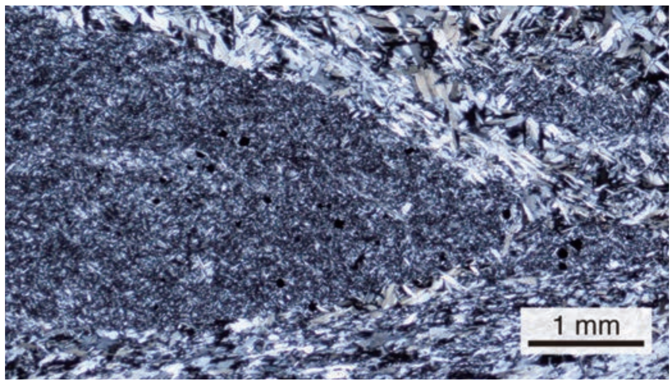

Fig. 2.
Photomicrograph (cross-polarized light) of serpentinite blocks surrounded by a serpentine (antigorite) matrix.

Introduction to Publicly Offered Research in Group C01

A model for depth-dependent slow earthquakes bridging geological and geophysical observations

Ryosuke ANDO, EPS, UTokyo

With the rapidly increasing number of geophysical observations of slow earthquakes, the depth-dependent modes of such earthquakes have been revealed systematically without depending on the details of the host tectonic environment. A typical example is found in the Nanka trough subduction zone. The deep slow earthquakes occur below the down-dip extension of seismogenic depth, with the shallower region of long-term slow-slip events (SSEs) occurring above the deeper region of short-term SSEs. Although many geological and physical models have been proposed for the mode of occurrence of slow earthquakes, we propose a general model that does not require specific metamorphic processes and material structures. This new model simulates the brittle—ductile heterogeneous fault zone structures observed at outcrops and considers the temperature dependences of two rheological properties, namely, the brittle fraction and viscosity. We analyze the model behavior with a one-degree-of-freedom spring-slider system. It is found that on the colder (shallower) side, slow but larger slip occurs, whereas on the warmer (deeper) side, relatively fast but smaller slip occurs. This behavior is understood in terms of the competition between the two rheological properties. The obtained behaviors appear to explain the observed depth dependence of the mode of slow earthquakes.

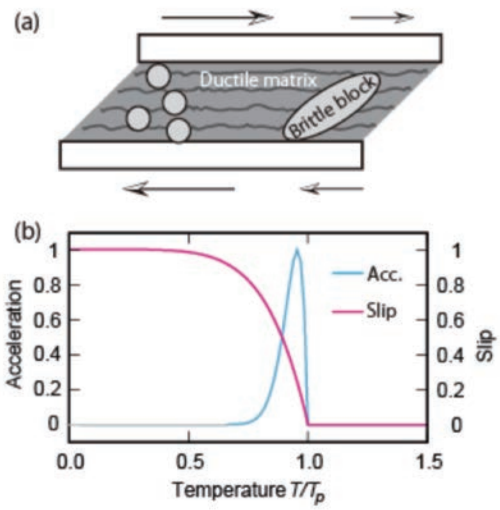

Fig. 1.
(a) Schematic illustration of fault zone structure. (b) Simulated temperature dependence of slip (purple) and acceleration (blue).

Introduction to Publicly Offered Research in Group C01

Geodetic slip inversion for long-term slow-slip events considering the model prediction errors originating from uncertainty in underground structure

Ryoichiro AGATA, JAMSTEC

Because long-term slow-slip events (L-SSEs) are of relatively long duration and large magnitude, we can estimate the slip distribution of L-SSEs using geodetic displacement data. Geodetic slip inversion requires a prior assumption of the underground structure. Given the uncertainty in the underground structure, the assumption of a single model of the underground structure may lead to large model prediction errors and in turn to significant bias in slip estimation results. To address this problem, we developed a new slip estimation method that incorporates the uncertainty in underground structure using an ensemble consisting of many models of underground structure. We applied the proposed method to estimate the distribution of slip in the L-SSE that occurred beneath the Bungo Channel during 2010. Commonly used slip inversion approaches impose prior empirical constraints on the parameters used for slip estimation to reduce the instability of estimation caused by sources of uncertainty. In contrast, the proposed method reduced the error associated with the "single model" assumption by considering multiple plate boundary models and elastic parameters simultaneously, and thus succeeded in estimating slip distribution that is consistent with other slow earthquakes in the surrounding area without the need for empirical constraints.

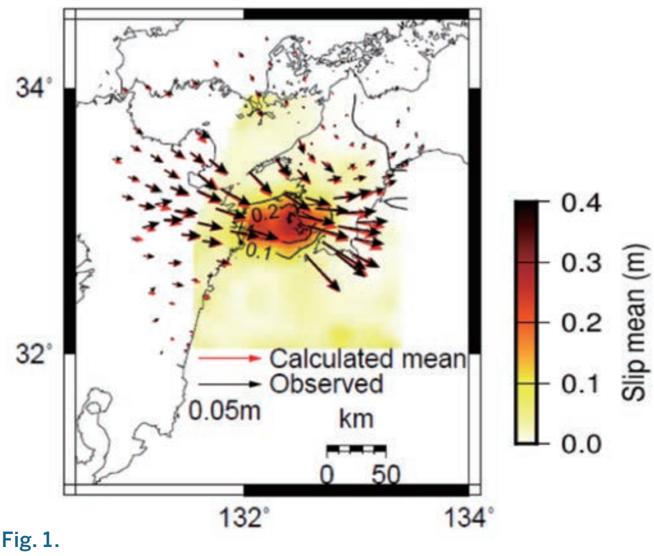

Fig. 1.
Obtained slip distribution of the 2010 L-SSE beneath the Bungo Channel.

Introduction to Publicly Offered Research in Group C02

Model experiments on the role of rough surfaces on the occurrence of fault slip

Atsuko NAMIKI, Nagoya Univ.

The surface of a subducting plate is not smooth and instead shows topographic variation (roughness). Such roughness may become an asperity, but it is not well understood how the roughness affects the occurrence of earthquakes. Therefore, a series of model experiments were conducted to visualize the fault slip on a fault plane with roughness. A gel was used to represent a hanging wall with a Maxwell fluid-like rheology, and an acrylic plate with a rough surface was used to represent a footwall. The stress relaxation of the gel generated an interlocked fault plane. By moving the acrylic plate, stress accumulated in the gel (**Fig. 1**). Eventually, the gel rebounded elastically and caused a rupture.

Experimental results show a correlation between the degree of roughness and the frequency of rupture occurrence. When the degree of roughness is high (**Fig. 1a**), both the stress that accumulated before the rupture and that released during the slip are large, and the occurrence frequency of ruptures is low. In contrast, when the degree of roughness is low, small, frequent ruptures occur (**Fig. 1b**). These results suggest that the degree of roughness can regulate the size and occurrence frequency of earthquakes.

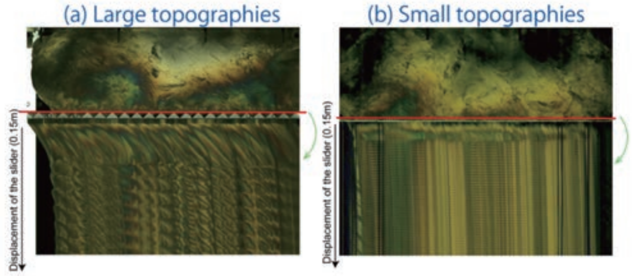

Fig. 1.
Time–space-dependent stress field of the hanging wall above a subducting plate with a rough surface, visualized by photoelasticity. The plate moves to the right. (a) and (b) show high and low degrees of roughness, respectively. The upper part in each panel shows the whole hanging wall, and the lower part shows the temporal (displacement) evolution of the stress fields in the range indicated by the red line. Horizontal lines appear as a result of the sudden elastic rebound of the hanging wall, indicating the occurrence of ruptures.

Science of Slow Earthquakes
Activity report

FY2020
Virtual WS

Virtual workshops/Slow Earthquakes WS 2020 Virtual

Kazushige OBARA, ERI, UTokyo

During the global spread of COVID-19 in 2020, we conducted several group seminars and workshops in virtual mode, utilizing various communication applications (14 April: C01, 25 March: C02, 16 and 23 June: A01/A02 joint, 28 July and 4 August: B01, 27 and 31 August: workshop for early career researchers, summer 2020). The WS for early career researchers was conducted with on-demand pre-recorded oral presentations and discussion on Slack, and was favorably received.

In 2020, the final year of the project, the International Joint Workshop on Slow Earthquakes was planned to take place in Nara, the ancient capital of Japan, with many invited speakers from overseas. Owing to restrictions on cross-border travel, the initial plan was changed, with a domestic virtual workshop (Slow Earthquakes WS 2020 Virtual) involving project members being run during 16–17 September. Given the experience with the WS for early-career researchers, the WS was implemented using on-demand content, such as pre-recorded oral presentations and virtual posters and discussion, on Slack and Zoom. Some presenters created their presentations using dictation software. There were 110 participants and 62 presentations.

More than 2000 messages were exchanged on Slack discussion during the WS. The virtual social party held during the evening of 16 September on Spatial Chat was a great success.

A post-WS survey showed that many of the participants were satisfied with the WS style, in which they could view presentations and ask questions whenever they liked. A few presenters had difficulty creating pre-recorded presentation content.

Because of the continuing difficulties caused by the COVID-19 pandemic, we plan to implement various types of workshops in virtual mode in the future.

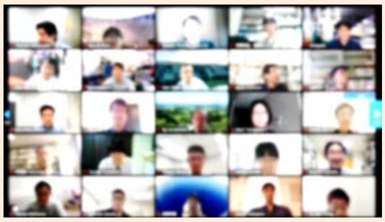

Science of Slow Earthquakes
Activity report

Report on the overseas dispatch of young researchers Ⅰ

Feb. 10 – Mar. 18, 2020
Overseas dispatch

Keisuke SATO, D2, Kobe Univ.

From February to March 2020, I attended the laboratory of Dr. Hideo Aochi of the Bureau de Recherches Géologiques et Minières (BRGM) and learned about dynamic rupture modeling of faults. This time, instead of modeling with a focus on the spatial distribution and detailed values of the parameters, we used previously obtained kinematic knowledge (static inversion using kinematic source inversion and crustal movement data). We discussed in detail the approach for establishing an approximate representation of rupture. By using only a limited number of observation points to calculate the mismatch between observed waveform and calculated waveform and reducing the range of dynamic rupture parameters to be searched, we aimed to obtain a rupture scenario while reducing the number of calculations. In future work, by comparing the location and amount of slip during an earthquake estimated by dynamic rupture modeling with the rupture area of a slow earthquake determined by previous research, we will compare the spatiotemporal space between regular earthquakes and slow earthquakes.

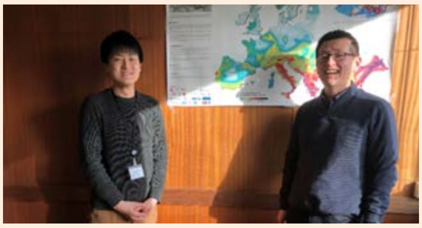

Science of Slow Earthquakes
Activity report

Report on the overseas dispatch of young researchers Ⅱ

Aug. 15, 2019 – Mar. 15, 2020
Overseas dispatch

Ayako TSUCHIYAMA, M2, Tokyo Tech.

I had the outstanding opportunity to launch a new research project with Prof. Roland Bürgmann and Dr. Taka'aki Taira at the University of California, Berkeley. We are working on the detection of low-frequency earthquakes (LFEs) in the 2019 Ridgecrest sequence and on the distribution of LFEs in time and space. I am grateful to have had a chance through this program to receive feedback from researchers in the United States, not only with respect to my research projects but also for my future academic career.

Science of Slow Earthquakes
Activity report

Workshop for early career researchers and students

Aug. 19 – 31, 2020
WS for young researchers

Naofumi ASO (Tokyo Tech.), Masayuki KANO (Tohoku Univ.),
Akiko TAKEO, Shunsuke TAKEMURA (ERI, UTokyo)

To obtain a better understanding of various aspects of slow earthquake phenomena, we held a workshop for early-career researchers during 30–31 January 2020 at Atami. Owing to the COVID-19 pandemic, we used online meeting tools after April. An on-demand-style workshop for early career researchers and students, including 13 presentations and 2 Zoom discussion sessions, was held during 19–31 August. We are continuing to hold online lunch meetings via Spatial Chat.

Science of Slow Earthquakes
Activity report

Jun.26, 2020
Online lab visit

Online laboratory visit

Yutaka SUMINO, Tokyo Univ. of Science

Most of the first half of 2020 was challenging, as we were essentially locked out of universities owing to COVID-19. During this difficult period, we utilized various online tools to allow discussion between people who were living in different locations. During early June, we restarted our laboratory activities. Given the situation, we organized an online (virtual) laboratory visit for 26 June to explore different perspectives on analog experiments related to slow earthquakes. Here I review the online laboratory visit and identify possible improvements.

It should be noted that the preparation for the online laboratory visit was somewhat easier than that for a regular site visit. Although some aspects of the preparation for the online site visit were the same as those for a regular site visit, the former does not have to consider visitor safety issues. Particular care was taken to show the details of experimental setups and facilities, with close-up video capture. The frame of view was adjusted to avoid participants being affected by possible excessive motion of the camera.

Several improvements could have been made to the online laboratory visit. The event was limited to the inside of our laboratory, but it should have started from the scenery outside the laboratory, such as a view of the campus, to simulate the feeling of a real (regular) visit. In addition, comments could not be obtained efficiently and easily from the participants. Furthermore, we should have avoided the lack of communication between our laboratory members and participants. One solution could have been to use a five-minute breakout room for small-group discussions between our laboratory members and participants. Frequent use of a breakout room function would have improved communication significantly. In a recent online lecture, we used a real-time whiteboard application, Miro, which could also have facilitated discussion between participants.

This online laboratory visit was a novel trial and allowed us to convey the laboratory atmosphere and demonstrate analog experiments without participants needing to commute long distances. It is hoped that this short note, reporting the online laboratory experience and possible improvements, will inform the planning for the next online laboratory visit and improve the degree of communication and collaboration between scientists.

Publisher/Contact

Office for Scientific Research on Innovative Areas:
Science of Slow Earthquakes
1-1-1 Yayoi, Bunkyo-ku, Tokyo, JAPAN 113-0032
(within the Earthquake Research Institute,The University of Tokyo)
TEL: +81-3-5841-2956
E-mail: sloweq-office@eri.u-tokyo.ac.jp

Date of issue 2021.Feb.

http://www.eri.u-tokyo.ac.jp/project/sloweq/en/

Science of Slow Earthquakes

Newsletter05